Materials Physics and Mechanics. 2023;51(1): 108-118
Research article
http://dx.doi.org/10.18149/MPM.5112023_10

Submitted: July 19, 2022
Approved: November 14, 2022
Accepted: January 18, 2023

Mechanical properties and deformation curves of the 3D-printed polycarbonate

I.K. Andrianov ✉, S.I. Feoktistov

Komsomolsk-na-Amur State University, Komsomolsk-on-Amur, Russia

✉ ivan_andrianov_90@mail.ru

Abstract. The aim of the study was to evaluate the mechanical characteristics of polycarbonate on the example of polycarbonate samples for 3D printing, to obtain the dependence of stress intensity on strain intensity taking into account compressibility. An experimental study of the mechanical properties of polycarbonate used in 3D printing has been carried out. Polycarbonate samples were made to perform tensile tests on a 3D printer. A series of stretching experiments were carried out in the elastic stage of samples to determine the Poisson's ratio of polycarbonate. To calculate the tensile strength, the conditional yield strength, polycarbonate samples were tested for rupture. Diagrams of conditional stresses from relative deformations are constructed. Since polycarbonate for 3D printing mainly works in the elasticity stage, the study constructed diagrams of polycarbonate deformation taking into account the compressibility of the material. According to the results of the study, the average values of the tensile elastic limit, the conditional yield strength, the tensile strength and the relative deformation at rupture of samples made by the 3d- printing method of polycarbonate were obtained. Deformations curves will allow us to estimate the stress-strain state of loaded polycarbonate elements not only under simple tension, but also under conditions of complex volumetric loading, since they relate the intensity of stresses and deformations.
Keywords: polycarbonate, deformation curve, 3D printing, stress, strain, compressibility

Acknowledgements. *The reported study was funded by the Russian Fund for Fundamental Research, project "Razrabotka modeli optimizacii form shtampovochnyh osnastok metodom effektivnogo pereraspredeleniya materiala", project number 19-38-60020\19.*

Citation: Andrianov IK, Feoktistov SI. Mechanical properties and deformation curves of the 3D-printed polycarbonate. *Materials Physics and Mechanics*. 2023;51(1): 108-118. DOI: 10.18149/MPM.5112023_10.

Introduction

The sustainable development of industry today involves the use of more economical and accurate methods of manufacturing products, one of such methods is the 3D prototyping method, which allows manufacturing parts for the aviation and automotive industries by printing on a 3D printer. The relevance of this direction lies in the possibility of switching from all-metal products to the manufacture of parts from polymers of optimized shape. However, it is important to assess the mechanical properties of polymers, in particular polycarbonate, which is actively used in 3D printing. Modern reference materials are mainly limited to the basic characteristics of the polymer, such as modulus of elasticity, yield strength, tensile strength. It is quite difficult to find stress dependence on polycarbonate deformations during loading, especially for samples obtained by 3D printing methods. Taking into account the compressibility of the material is important, since polycarbonate used for 3D

Publisher: Peter the Great St. Petersburg Polytechnic University

furnaces practically does not work in the field of plastic deformation, respectively, in the field of elasticity, it is necessary to determine experimentally the value of the Poisson's ratio and take into account when constructing the dependence of stress intensity on strain intensity.

According to the literature review, the issues of sustainable development of domestic industry at the present stage require solving a large number of engineering problems, which is noted in [1]. Modern production automation systems and the design of complex structures are mainly associated with the use of metals [2-4]. At the same time, the transition to the use of polymers in the production of parts is one of the vectors of sustainable development. Issues related to the study of the mechanical and thermal properties of polycarbonate for 3D furnaces were investigated in [5-10]. Structural models and chemical features of the properties of substances used in industry are investigated in [11-13]. A feature of the use of polymers in industry is the possibility of reuse. The problems of recycling of secondary raw materials were investigated in the works [14, 15].

Since many products experience prolonged loads during operation, accompanied by the appearance of fatigue defects, it is important to assess cyclic loads, fatigue failure [16-18]. Experimental studies of the creep and dynamic properties of polycarbonate are presented in [19]. In addition, the peculiarity of polymers is that in the process of cyclic deformation, self-heating phenomena may occur. The problems of temperature modeling, optimization of polymer structures in self-heating conditions are presented in [20-23]. The problems of finite element simulation related to the assessment of the stress-strain state are considered in studies [24-28]. The issues of studying the mechanics of plastics and composite materials are investigated in the works [29-31].

Methods

The purpose of the study was to construct a diagram of polycarbonate deformation taking into account the compressibility of the material. The peculiarity of the deformation diagram is that it relates the intensity of stresses and the intensity of deformations, in contrast to the diagram for simple stretching. Therefore, the deformation diagram can be used in the study of the volumetric stress state of the elements. Taking into account the compressibility of polycarbonate will allow taking into account the influence of the elastic component of deformation when assessing the stress-strain state.

To achieve this goal, it was necessary to consider a number of subtasks, namely:

- conduct a full-scale experiment on simple stretching of samples made of polycarbonate by 3D printing until destruction;
- build a diagram of conditional stresses;
- to conduct a full-scale experiment on simple stretching in order to calculate the Poisson's ratio when loaded to the yield point;
- construct a deformation diagram for true stresses and logarithmic deformations with and without taking into account the compressibility of the material.

When constructing the polycarbonate deformation diagram, it was necessary to switch to true stresses and logarithmic deformations. This step is due to the need to take into account the change in the cross-sectional area of the sample during deformation, since the conditional stress diagram is constructed under the assumption that the cross-sectional area remains unchanged, while in the process of simple stretching, the transverse dimensions of the sample decrease. Since samples made of polymers by 3D printing methods can be used under repeated loads, it is necessary to take into account the need for summation of deformations. Since relative deformations do not have the additivity property, we will construct the diagram using logarithmic deformations that have the summation property.

To switch to true stresses, taking into account the reduction of the cross-sectional area, we use the condition:

$$\sigma_s F = \sigma F_0, \quad (1)$$

where σ_s – true stresses, F – current cross–sectional area, σ – conditional stresses, F_0 – initial cross-sectional area of the sample.

Taking into account the incompressibility condition $F_0 l_0 = Fl$, the true stresses are determined through the relative longitudinal strain ε and conditional stresses according to (1):

$$\sigma_s = \sigma(1 + \varepsilon), \quad (2)$$

To determine the true stresses, taking into account the compressibility of the material, consider the change in the geometric characteristics of the sample: thickness *a*, width *b* and length *l*. Let the dimensions of the body change after deformation according to the ratios:

$$a = a_0(1 + \varepsilon_\perp),\ b = b_0(1 + \varepsilon_\perp),\ l = l_0(1 + \varepsilon), \quad (3)$$

where a_0 – the initial thickness, b_0 – the initial width, l_0 – the initial length, $\varepsilon_\perp$ – relative transverse strain.

The initial cross-sectional area is determined by $F_0 = a_0 b_0$. After deformation, the cross-sectional area will change according to (3):

$$F = ab = F_0(1 + \varepsilon_\perp)^2. \quad (4)$$

We express the cross-sectional area (4) in terms of the coefficient of transverse strain:

$$\mu' = -\frac{e_\perp}{e}, \quad (5)$$

where $e = \ln(1 + \varepsilon)$ – logarithmic longitudinal deformation, $e_\perp = \ln(1 + \varepsilon_\perp)$ – logarithmic transverse strain.

We express the transverse relative deformation in terms of the coefficient of transverse deformation according to (5):

$$\varepsilon_\perp = exp(-e\mu') - 1. \quad (6)$$

Substituting (6) into (4), we obtain a change in the cross-sectional area taking into account the compressibility of the material:

$$F = F_0 \exp(-2\mu' e). \quad (7)$$

Then the true stresses according to (1), (7) are determined through the coefficient of transverse deformation:

$$\sigma_s = \sigma \exp(2\mu' e). \quad (8)$$

The coefficient of transverse deformation is determined according to [29]

$$\mu' = \frac{1}{2} - \frac{(1-2\mu)}{2E}\frac{\sigma_s}{e}. \quad (9)$$

Taking into account (9), the true stresses (8), taking into account the compressibility of the material, will be determined:

$$\sigma_s = \sigma \exp\left(e - \frac{1-2\mu}{E}\sigma_s\right). \quad (10)$$

Since the true stresses cannot be expressed explicitly in terms of logarithmic deformations and conditional stresses, we substitute in the right part (10) the value of the true stress obtained without taking into account compressibility:

$$\sigma_s \approx \sigma \cdot \exp(e),$$

then the true stress is determined by

$$\sigma_s = \sigma \exp\left(e - \frac{1-2\mu}{E}\sigma \cdot \exp(e)\right) \quad (11)$$

To construct a deformation diagram, imagine the intensity of logarithmic deformations [32]:

$$e_i = \frac{\sqrt{2}}{3}\sqrt{(e_1 - e_2)^2 + (e_2 - e_3)^2 + (e_3 - e_1)^2} \quad (12)$$

where e_1, e_2, e_3 – main logarithmic strains:

$$e_1 = e,\ e_2 = e_3 = -\mu' e. \quad (13)$$

Substitute the relations (9), (13) in (12), then the intensity of deformations is expressed in terms of longitudinal deformation by the ratio:

$$e_i = e - \frac{(1-2\mu)}{3E}\sigma_s,$$

because $\sigma_s = \sigma_i$ – the intensity of the stresses, we get

$$e_i = e - \frac{(1-2\mu)}{3E}\sigma_i. \quad (14)$$

In the elasticity stage , the dependence of the intensity of deformations on the intensity of stresses will take the form:

$$e_i = \frac{2(1+\mu)}{3E}\sigma_i, \ e_i \le e_{iT} \quad (15)$$

In the case of an incompressible material $(\mu = 0.5)$ the deformation diagram and the true stress diagram according to (15) coincide. As a result, the deformation diagram $\sigma_i - e_i$ can be presented in parametric form according to the diagram $\sigma_s - e$:

$$\begin{cases} \sigma_i = \sigma_s \\ e_i = e - \dfrac{(1-2\mu)}{3E}\sigma_s \end{cases}.$$

Thus, according to the discrete data of the diagram of conditional stresses σ from relative deformations ε, the construction of the deformation diagram will be determined by the relations:

$$\sigma_i = \sigma\exp\left(\ln(1+\varepsilon) - \frac{1-2\mu}{E}\sigma(1+\varepsilon)\right), \quad (16)$$

$$e_i = \ln(1+\varepsilon) - \frac{(1-2\mu)}{3E}\sigma\exp\left(\ln(1+\varepsilon) - \frac{1-2\mu}{E}\sigma(1+\varepsilon)\right). \quad (17)$$

Results and Discussion

To conduct a simple stretching experiment, samples made by 3D printing from polycarbonate on a Designer X printer of the Picaso3D brand were used (Figure 1). The tests were carried out according to the methodology described in [33]. When printing samples, the Fused Filament Fabrication technology was used.

Fig. 1. Simple stretching of a sample made of polycarbonate by 3D printing

To calculate the Poisson's ratio, the tensile force loading was carried out within elastic deformations. The stress from the external load was 25 MPa. The initial geometric characteristics of the cross-section of the sample are presented in Table 1. Measurements of the thickness and width of the cross-section were carried out twice at 5 points along the length of the sample. The results of thickness and width measurements before the start of the tests are presented in Table 1. The length of the sample before and after the test: $l_0 = 120\ mm, l = 121.425\ mm$.

Table 1. Geometric characteristics of the cross-section of the sample before deformation

№ point	Thickness, mm		Width, mm	
	First dimension	Second dimension	First dimension	Second dimension
1	4.258	4.258	10.429	10.422
2	4.278	4.273	10.321	10.315
3	4.321	4.315	10.227	10.227
4	4.355	4.358	10.209	10.208
5	4.403	4.401	10.22	10.215

The arithmetic mean values of the thickness $\bar{a}$ and width $\bar{b}$ of the sample were determined by the formulas:

$$\bar{a} = \frac{1}{10}\sum_{i=1}^{10} a_i\,, \qquad \bar{b} = \frac{1}{10}\sum_{i=1}^{10} b_i.$$

Accordingly, the average values of thickness and width before the sample test were obtained:

$\bar{a} = 4{,}32\ mm, \qquad \bar{b} = 10.28\ mm$

The average quadratic error of measuring the average thickness and width of the sample was determined by the formulas:

$$S_{\bar{a}} = \sqrt{\sum_{i=1}^{10} \frac{(a_i - \bar{a})^2}{90}}, \quad S_{\bar{b}} = \sqrt{\sum_{i=1}^{10} \frac{\left(b_i - \bar{b}\right)^2}{90}}$$

$S_{\bar{a}} = 0.018\,, \qquad S_{\bar{b}} = 0.028$

For the confidence probability $\alpha = 0{,}98$, the Student's coefficient was assumed to be equal to $t_\alpha = 3{,}7$. As a result, the average values of the cross-section of the sample with a confidence interval were assumed to be equal: $a = 4{,}32 \pm 0.065\ mm,\ b = 10{,}28 \pm 0.102\ mm$.

The relative measurement errors are equal to: $\delta_{\bar{a}} = 1{,}5\%,\ \delta_{\bar{b}} = 1\%$.

The results of measurements of the thickness and width of the sample after stretching are presented in Table 2.

Table 2. Geometric characteristics of the cross-section of the sample after deformation

№ point	Thickness, mm		Width, mm	
	First dimension	Second dimension	First dimension	Second dimension
1	4.249	4.240	10.360	10.352
2	4.251	4.259	10.264	10.239
3	4.289	4.295	10.161	10.169
4	4.329	4.330	10.171	10.165
5	4.382	4.369	10.177	10.173

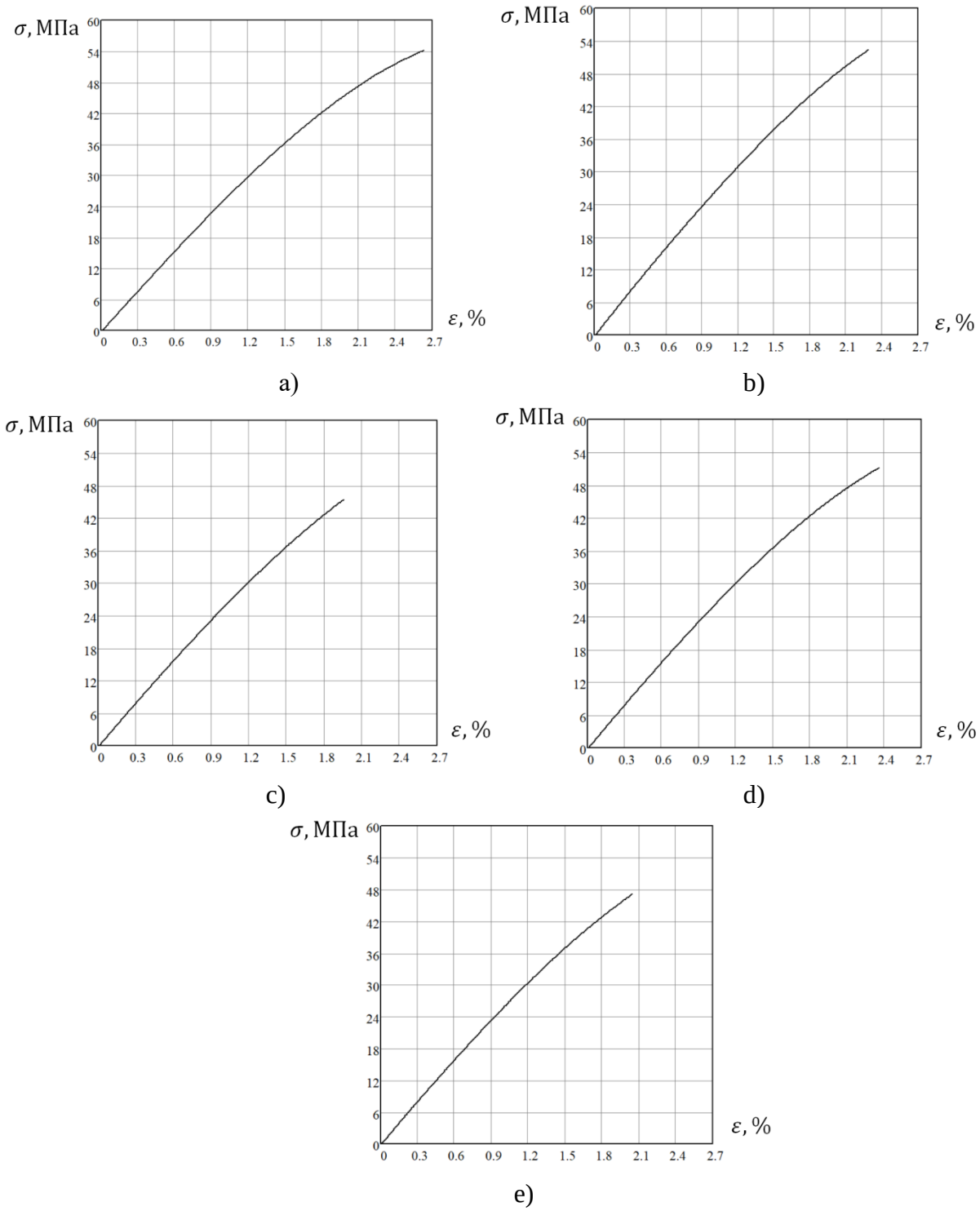

Fig. 2. Diagram of the dependence of the conditional stresses on the relative strains of polycarbonate: a) sample 1, b) sample 2, c) sample 3, d) sample 4, e) sample 5

The average quadratic error of measuring the average thickness and width of the sample after deformation:

$S_{\bar{a}} = 0.01$, $S_{\bar{b}} = 0.025$

The average values of the thickness and width of the sample after deformation with a given confidence interval:

$a = 4.30 \pm 0.06\ mm,$ $b = 10.22 \pm 0.09\ mm,$

The relative measurement errors are equal to:

$\delta_{\bar{a}} = 1.4\%, \qquad \delta_{\bar{b}} = 0.8\%$

Poisson's ratio according to (5) when changing the thickness and width of the sample in the experiment for simple stretching:

$$\mu_a = 0.41, \ \mu_b = 0.46 \tag{18}$$

According to the calculated values (18), the average value of the Poisson's ratio of polycarbonate under simple tension is determined:

$$\mu = 0.44 \tag{19}$$

Based on the results of the simple stretching experiment, a diagram of the dependence of conditional stresses on relative deformations was taken for 5 different samples (Figure 2).

Table 3 shows the values of the mechanical characteristics of 5 samples: tensile modulus of elasticity, conditional yield strength, tensile strength, relative deformation at the moment of rupture.

Table 3. Mechanical properties of polycarbonate based on the results of a simple stretching experiment.

Modulus of elasticity, MPa	Conditional yield strength, MPa	Tensile strength, MPa	Relative strain at the break, %
2602	42.24	54.17	2.64
2756	43.45	52.28	2.28
2679	41.96	45.40	1.96
2687	40.98	51.17	2.36
2719	41.23	47.11	2.05

The deformation diagram (Figure 3), taking into account and without taking into account the compressibility of the material, was constructed according to the ratios (20), (21), (25) according to the diagrams of conditional stresses (Figure 2).

Thus, according to the results of the conducted experiments on rupture and stretching in the field of elasticity, the average values of the main mechanical characteristics of polycarbonate used for 3D printing were determined: the elastic modulus at tension, the conditional yield strength, the tensile strength, the relative deformation at the moment of rupture, the Poisson's ratio (table 4).

Table 4. Mechanical properties of polycarbonate based on the results of a simple stretching experiment.

Mechanical characteristics of polycarbonate for 3D printing	Average values
Tensile modulus of elasticity	2689 MPa
Conditional yield strength	41.97 MPa
Tensile strength	50.03 MPa
Relative strain at break	2.26 %
Poisson's Ratio	0.44

Deformation diagrams were obtained for 5 samples made by 3D printing from polycarbonate with and without compressibility. Comparing the results in Figures 1 and 2, it should be noted that the maximum error when using a conditional stress diagram instead of a deformation diagram is 5 %; failure to take into account the compressibility of the material during deformation leads to an error of 2 %.

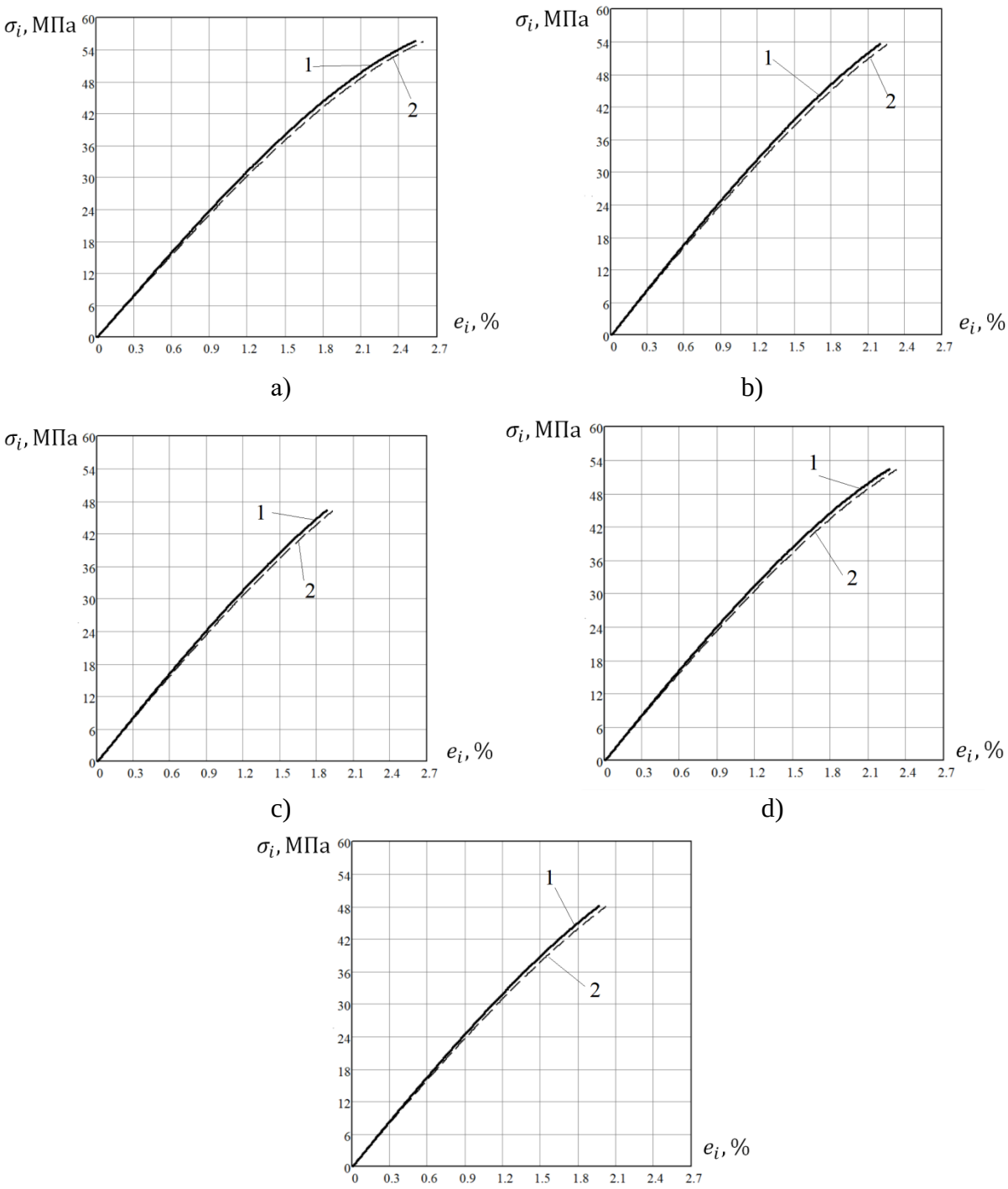

1 – taking into account the compressibility of the material, 2 – without taking into account the compressibility of the material

Fig 3. Polycarbonate deformation diagram: a) sample 1, b) sample 2, c) sample 3, d) sample 4, e) sample 5

Conclusion

The results of the study make it possible to increase the efficiency of industrial production, since the obtained deformation diagrams can be used to assess the stress-strain state of manufactured parts for aviation and automotive purposes by 3D prototyping methods made of polycarbonate. This approach creates the necessary prerequisites for the sustainable development of industry, since the use of polymers instead of metals in the manufacture of parts will allow for more accurate production except for the costs of finishing work.

References

1. Shakirova OG, Bashkov OV, Khusainov AA. Future challenges on the way to industrial development of equipment and technologies in the digital economy and industry 4.0 (conclusion). In: *Current Problems and Ways of Industry Development: Equipment and Technologies. Lecture Notes in Networks and Systems*. Cham; Springer; 2021. p.1063–1064.
2. Kosmynin AV, Schetinin VS, Khvostikov AS, Smirnov AV. Design of high-speed rotor systems with gas-magnetic bearings. In: Shakirova OG, Bashkov OV, Khusainov AA. (eds) *Current Problems and Ways of Industry Development: Equipment and Technologies. Lecture Notes in Networks and Systems*. Cham: Springer; 2021. p.597-604.
3. Mokritskii BJ, Shelkovnikov VY. Turning and milling conceptual issues. In: Shakirova OG, Bashkov OV, Khusainov AA. (eds) *Current Problems and Ways of Industry Development: Equipment and Technologies. Lecture Notes in Networks and Systems*. Cham; Springer; 2021. p.538-547.
4. Sukhorukov S, Mokritskiy B, Morozova A. Development of a Security Subsystem of a Robotic Laser Welding Complex. In: Radionov AA, Gasiyarov VR. (eds) *Advances in Automation II. RusAutoCon 2020. Lecture Notes in Electrical Engineering*. Cham; Springer; 2021. p.642–652.
5. Pramod T, Jaiprakash N, Sampathkumaran P. Influence of Betel Nut Concentration in the Matrix of Polycarbonate and ABS on the Mechanical Characteristics. In: Vinyas M, Loja A, Reddy K. (eds) *Advances in Structures, Systems and Materials. Lecture Notes on Multidisciplinary Industrial Engineering*. Singapore: Springer: 2019. p.267-275.
6. Sabet M, Mohammadian E. The inclusion of graphene nanoplatelet on the mechanical, thermal, and electrical characteristics of polycarbonate. *Polymer Bulletin*. 2022;15: 1-17.
7. Wu C, Chen C, Chen P. Characteristics of Polycarbonate Soft Segment-Based Thermoplastic Polyurethane. *Applied Sciences*. 2021;11: 5359.
8. Liu Y, Lu X. Chemical recycling to monomers: Industrial Bisphenol-A-Polycarbonates to novel aliphatic polycarbonate materials. *Journal of Polymer Science*. 2022;60(24): 3256-3268.
9. Yongsheng E, Yang F. Study on Synthesizing Polycarbonate with Triphosgene. *Journal of Physics: Conference Series*. 2022;2194: 012033.
10. Bahar A, Belhabib S. Mechanical and Thermal Properties of 3D Printed Polycarbonate. *Energies*. 2022;15(10): 3686.
11. Shakirova OG, Naumov DY, Lavrenova LG, Petkevich SK, Potkin VI. Structural identification of the new binuclear Cu(II) complex with unexpected nitration of a ligand. *Inorganic Chemistry Communications*. 2021;133: 108957.
12. Shakirova OG. Thermally induced spin crossover in iron (ii, iii) complexes with tripodal ligands. In: Shakirova OG, Bashkov OV, Khusainov AA. (eds) *Current Problems and Ways of Industry Development: Equipment and Technologies. Lecture Notes in Networks and Systems*. Cham: Springer; 2021. p.319-330.
13. Shabalin YA, Sarilov MY, Shakirova OG. Demercaptanization of straight-run kerosene fraction according to “demerus jet” technology. In: Shakirova OG, Bashkov OV, Khusainov

AA. (eds.) *Current Problems and Ways of Industry Development: Equipment and Technologies. Lecture Notes in Networks and Systems.* Cham: Springer; 2021. p.310-318.
14. Kolesnikov AS, Zhakipbaev B, Zhanikulov NN, Kolesnikova OG, Akhmetova YK, Kuraev RM, Shal AL. Review of technogenic waste and methods of its processing for the purpose of complex utilization of tailings from the enrichment of non-ferrous metal ores as a component of the raw material mixture in the production of cement clinker. *Rasayan Journal of Chemistry*. 2021;14(2): 997-1005.
15. Kolesnikov AS, Serikbaev BE, Zolkin AL, Kenzhibaeva GS, Isaev GI, Botabaev NE, Shapalov SK, Kolesnikova OG, Iztleuov GM. Processing of Non-Ferrous Metallurgy Waste Slag for its Complex Recovery as a Secondary Mineral Raw Material. *Refractories and Industrial Ceramics.* 2021;62(4): 375-380.
16. Andrianov IK. Modeling of Forming Die Under Cyclic Loading Conditions. In: *2020 International Multi-Conference on Industrial Engineering and Modern Technologies*. IEEE; 2020. p.20212072.
17. Andrianov IK. Finite Element Calculation of the Polymer Stamp Material Redistribution Under Restrictions on Fatigue Life. *Materials Science Forum*. 2022;1049: 248–254.
18. Andrianov IK, Grinkrug MS, Vakuluk AA. Numerical calculation of the heat sink parameters of the shell turbine vanes at the modeling of the heat-protective coating with a different number of layers. In: Shakirova OG, Bashkov OV, Khusainov AA. (eds) *Current Problems and Ways of Industry Development: Equipment and Technologies. Lecture Notes in Networks and Systems*. Cham; Springer: 2021. p.37-46.
19. Mu Q. Experimental data for creep and dynamic mechanical properties of polycarbonate and polycarbonate. *Data in Brief*. 2022;42: 108264.
20. Andrianov IK. Rod-Based Model for Optimization of a Polymer Die with Self-Heating in Cyclic Loading. *Russian Engineering Research*. 2021;41: 403-406.
21. Andrianov IK. Optimization Model of Thermal Loading of Multilayer Shells Based on the Strength Criterion. In: *2019 International Multi-Conference on Industrial Engineering and Modern Technologies*. IEEE; 2019. p.19229158.
22. Tupitsin M, Trishkina I, Sycheva S, Storozheva E, Novikov R. Study of the influence of structural heritage and operating conditions on the durability of safety valve springs from steel 50KHFA. *Materials Physics and Mechanics*. 2022;48(2): 161-174.
23. Kolesnikov AS, Sergeeva IV, Botabaev NE, Al'Zhanova AZ, Ashirbaev KA. Thermodynamic simulation of chemical and phase transformations in the system of oxidized manganese ore – carbon. *Izvestiya Ferrous Metallurgy*. 2017;60(9): 759–765.
24. Mokritskii B, Morozova A, Sitamov EJ. Simulation Modeling of the Choice of Metal Cutting Tool Coating. In: Radionov AA, Gasiyarov VR. (eds) *Proceedings of the 6th International Conference on Industrial Engineering (ICIE 2020). ICIE 2021. Lecture Notes in Mechanical Engineering*. Cham; Springer: 2021. p.156-162.
25. Andrianov IK. Topological optimization of a complex shape forming stamp. *Journal of Physics: Conference Series*. 2021;2096: 012115.
26. Andrianov IK. Modification of the stamp topological optimization taking into account cyclic fatigue based on the finite element approach. *International Journal of Mechanics*. 2021;15: 145–150.
27. Andrianov IK, Stankevich A. The stress-strain state simulation of the aircraft fuselage stretch forming in the ANSYS. *Journal of Physics: Conference Series*. 2019;1333: 082002.
28. Mokritskii BY, Shakirova OG, Sosnin AA, Sitamov ES, Erukov AI. Estimation of the Results of Predictive Simulation of a Rational Cutting Material. *Russian Metallurgy*. 2020;13: 1613–1618.
29. Pogrebnoi AV. Study of polylactide 3D-printed samples with double-layer weave. *Materials Physics and Mechanics*. 2022;48(2): 289-299.

30. Mzad H. Experimental investigation of the mechanical behavior of honeycomb sandwich composite under three-point bending fatigue. *Materials Physics and Mechanics*. 2022;48(2): 217-231.
31. Belaziz A, Mazari M, Bouamama M, Zahaf S, Mouloud D. Experimental study of ductile and fragile pipe cracked in High-Density Polyethylene (HDPE). *Materials Physics and Mechanics.* 2022;48(2): 199-207.
32. Malinin, N.N. *Applied theory of plasticity and creep*. 1975. (In-Russian)
33. International Organization for Standardization. ISO 527-2:2012. *Plastics - Determination of tensile properties*. 2018.

THE AUTHORS

Andrianov I.K.
e-mail: ivan_andrianov_90@mail.ru

Feoktistov S.I.
e-mail: serg_feo@mail.ru